ANL/HEP 7336
July 1973

Differential Cross Sections in $\pi^- p \to K^0 \Lambda^0$ and $\pi^- p \to K^0 \Sigma^0$ from 3 to 6 GeV/c†

C. E. W. Ward, I. Ambats, A. Lesnik*, W. T. Meyer, D. R. Rust**, and D. D. Yovanovitch***

Argonne National Laboratory
Argonne, IL 60439

---

† Based on a thesis submitted by Abraham Lesnik to the Faculty of the Department of Physics of the University of Chicago, in partial fulfillment of the requirements for the Ph D degree. This work was supported by the U. S. Atomic Energy Commission.

* Present address: Dept. of Physics, Ohio State University, Columbus, OH 43210.

** Present address: Dept. of Physics, Indiana University, Bloomington, IN 47401.

*** Present address: National Accelerator Laboratory, P.O. Box 500, Batavia, IL 60510.

Abstract

We have measured the differential cross sections for the associated production reactions $\pi^- p \rightarrow K^o \Lambda^o$ and $\pi^- p \rightarrow K^o \Sigma^o$ at 3, 4, 5, and 6 GeV/c, with a total of over 40,000 events. We find that both reactions have exponential forward peaks for $-t \cdot 0.4$ $(GeV/c)^2$, with no indication of forward direction flattening or turnover; the slopes of the forward peaks show little if any variation with momentum; and the two cross sections are equal within experimental error from $-t = 1.2$ $(GeV/c)^2$ out to at least $-t = 2.0$ $(GeV/c)^2$.

Knowledge of the associated production reactions $\pi^- p \rightarrow K^o \Lambda^o$ and $\pi^- p \rightarrow K^o \Sigma^o$ at high energies is important for the amplitude analysis of hypercharge exchange processes. Such an analysis requires high quality data, and in this paper we present differential cross section measurements of these processes made at 3, 4, 5, and 6 GeV/c, with a total data sample of over 40,000 events.

This experiment was performed at the Argonne ZGS accelerator, using the Argonne Effective Mass Spectrometer. The technique of the experiment was to detect the $\pi^+ \pi^-$ decay of the K^o_s's produced in the forward direction. The momentum of the decay pions was measured, and the $K^o \Lambda^o$ and $K^o \Sigma^o$ reactions were separated by means of the calculated missing mass.

The experimental apparatus is shown in Figure 1. A beam of typically 200,000 π^- per pulse was focussed on an 8 inch long liquid hydrogen target. An array of counters at an intermediate focus tagged the momentum of each particle to a precision of $\pm 0.27\%$. Four threshold Cherenkov counters identified each beam particle as π^-, K^-, or $\bar{p}$. The hydrogen target was followed by a 5-inch by 10-inch array of veto counters, used to veto events with charged particles emerging downstream of the target. Wire spark chambers with magnetostrictive readout were located in front of, behind, and inside the large aperture of the Effective Mass Spectrometer to provide measurements of the particle trajectories. Another set of three wire chambers was used to measure the beam particle position and angles. An on-line EMR-6050 computer wrote the raw data onto magnetic tape for later processing, performed

checks of the experimental apparatus, and performed preliminary physics calculations.

Neutral V-particle decays were selected by requiring total anti-coincidence in the veto counter array, followed by charged particles producing a signal in counter CM located 20 inches further downstream. Two or more counts were required in a 40-element counter hodoscope located behind the magnet to ensure that both charged particles from a V-particle decay passed through the magnet aperture.

For π^--induced events with at least one fitted track of each charge, pion masses were assumed for each pair of particles and the $\pi^+\pi^-$ effective mass was calculated. A peak with an RMS width of 3 MeV/c^2 was found at the K^o mass. Events in the peak region were fitted to the hypothesis $K^o \rightarrow \pi^+\pi^-$ and the missing mass squared of each event was calculated, resulting in the distributions shown in Figure 2. The good resolution was due in large part to the use of spark chambers inside the spectrometer magnet. A good $\Lambda^o - \Sigma^o$ separation could be made at all momenta by appropriate cuts on the missing mass distributions.

Corrections were made as a function of $t' = t - t_{min}$ for loss of events outside the missing mass cuts and for cross-contamination between Λ^o and Σ^o regions (about a 10% effect in the worst case, at 6 GeV/c). Acceptance corrections were made through the use of a Monte Carlo program which took into account the decays of both V-particles in the reaction as well as the energy loss and multiple Coulomb scattering of decay products in the liquid

hydrogen and the target structural materials.

Systematic corrections were made for the $K^{o} \rightarrow \pi^{+}\pi^{-}$ branching ratio, target empty effects (typically 5%), beam contamination by e^{-} and μ^{-} (5%), loss of events rejected in the analysis because they had been tagged by the electronics as having a later beam track passing through the apparatus within the resolving time of the spark chambers (22%), analysis program efficiency (5%), accidental and dead-time effects (3%), and a number of other smaller effects. Contamination by forward-produced kinematically ambiguous Λ^{o} particles was very small (typically 0.25%), and contamination with $e^{+}e^{-}$ pairs from converted gamma rays was negligible.

The resulting differential cross sections are presented in Figure 3 and Table 2. We estimate possible systematic overall scale errors of ± 10%, with no more than ± 3% scale error variation between results at different beam momenta. The cross sections are in excellent agreement with previous measurements of these reactions.[1]

The features of the data are similar at all four momenta. Each cross section has an exponential forward peak, followed by a break near $t' = -0.4$ $(GeV/c)^2$. There is no evidence for flattening or turn-over in the forward direction, indicating the dominance of non-spin-flip production mechanisms in both reactions. The result of a fit of the forward cross sections to the form $d\sigma/dt = Ae^{Bt'}$ are given in Table 1. The slopes of the forward peaks in both the $K^{o}\Lambda^{o}$ and $K^{o}\Sigma^{o}$ reactions do not vary rapidly with beam momentum from 3 to 6 GeV/c and are quite consistent with those found by Foley et al.,[2]

at 8, 10.7, and 15.7 GeV/c. It would appear that there is little if any variation of the forward slopes over the full range from 3 to 16 GeV/c. The $K^{o}\Lambda^{o}$ forward cross section is found to be less steep at all momenta, indicating a relatively larger spin-flip production amplitude than for the $K^{o}\Sigma^{o}$ reaction.

The cross section beyond the break at $t' = -0.4$ $(GeV/c)^2$ is relatively flat for $K^{o}\Sigma^{o}$, but less so for $K^{o}\Lambda^{o}$. At 4 GeV/c and above the cross sections are observed to converge to a common value near $t' \approx -1.2$ $(GeV/c)^2$, remaining approximately equal out to at least $t' = -2.0$ $(GeV/c)^2$.

Our cross sections for $\pi^{-}p \rightarrow K^{o}\Sigma^{o}$ may be compared with those for $\pi^{+}p \rightarrow K^{+}\Sigma^{+}$, assuming pure I = 1/2 exchange, by means of the relation $d\sigma/dt(\pi^{-}p \rightarrow K^{o}\Sigma^{o}) = (1/2)\, d\sigma/dt(\pi^{+}p \rightarrow K^{+}\Sigma^{+})$. Using existing data on $\pi^{+}p \rightarrow K^{+}\Sigma^{+}$ [3, 4, 5], we find that our data is in good agreement at 4 GeV/c and above with the predictions of pure I = 1/2 exchange.

At 3 GeV/c, the I = 1/2 exchange relation is not well satisfied if we compare to the 3.0 and 3.25 GeV/c data of Pruss et al.[3] We do not see the rapid increase with energy of the forward cross section slope reported in that paper. A sharp change of slope near $t = -0.1$ $(GeV/c)^2$ in the 3 GeV/c $\pi^{+}p \rightarrow K^{+}\Sigma^{+}$ cross section has been inferred by Kalbaci et al.[4], using their data combined with that of Pruss et al. We see no sign of such structure, even though the range of t covered by our data spans that of both $K^{+}\Sigma^{+}$ experiments.

We would like to thank our collaborators in the construction of the Effective Mass Spectrometer: R. Diebold, D. Ayres, A. F. Greene, S. L. Kramer, and A. B. Wicklund. We also wish to thank R. Ely and C. Klindworth for maintaining and repairing the EMR-6050 computer, and R. Rivetna for aiding with the computer programming. Finally, we are indebted to all the ZGS operating personnel for their continuing support during all phases of the experiment.

References

1. O. I. Dahl et al., Phys. Rev. 163, 1430 (1967); M. Abramovich et al., Nuclear Phys. B27, 477 (1971); D. J. Crennell et al., Phys. Rev. D6, 1220 (1972).

2. K. J. Foley et al., Physical Review D (to be published).

3. S. M. Pruss et al., Phys. Rev. Letters 23, 189 (1969).

4. P. Kalbaci et al., Phys. Rev. Letters 27, 74 (1971).

5. A. Bashian et al., Phys. Rev. D4, 2667 (1971).

Figure Captions

1. The Argonne Effective Mass Spectrometer.

2. Missing mass squared distributions from $\pi^- p \rightarrow K^o X$.

3. Differential cross sections for $\pi^- p \rightarrow K^o \Lambda^o$ and $\pi^- p \rightarrow K^o \Sigma^o$.

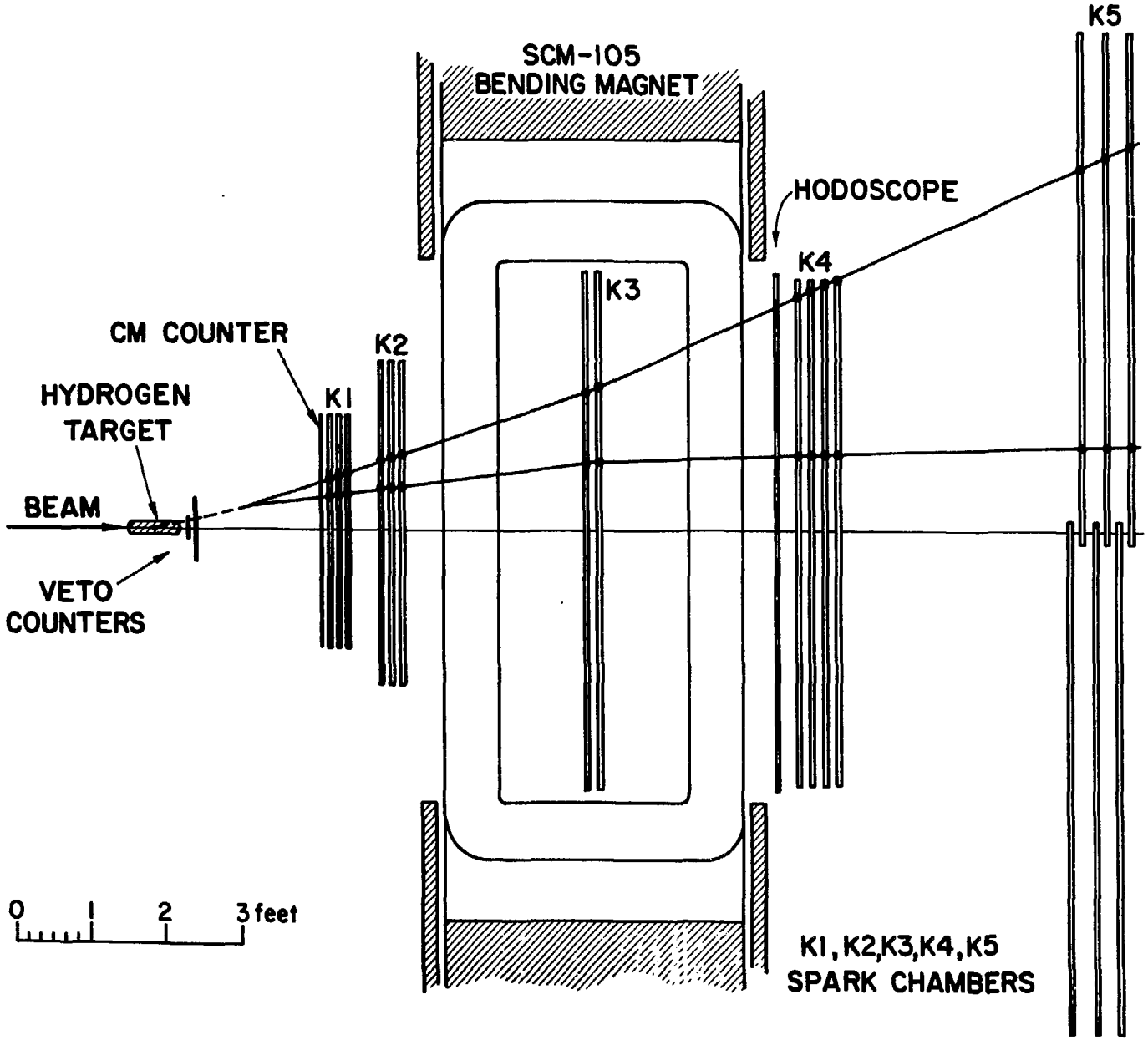
K5
SCM-105
BENDING MAGNET
HODOSCOPE
K4
K3
CM COUNTER
K2
HYDROGEN
TARGET
K1
BEAM
VETO
COUNTERS
0
1
2
3 feet
K1, K2, K3, K4, K5
SPARK CHAMBERS

Figure 1

$\pi^- p \rightarrow K^\circ X$
MISSING MASS
6 GeV/c
16,094 EVENTS
5 GeV/c
8979 EVENTS
4 GeV/c
13,137 EVENTS
3 GeV/c
5708 EVENTS
EVENTS
1200
800
400
0
400
200
0
800
400
0
400
200
0
Λ°
Σ°
1.0
1.1
1.2
1.3
1.4
1.5
1.6
M_X^2, $(GeV/c^2)^2$

Figure 2

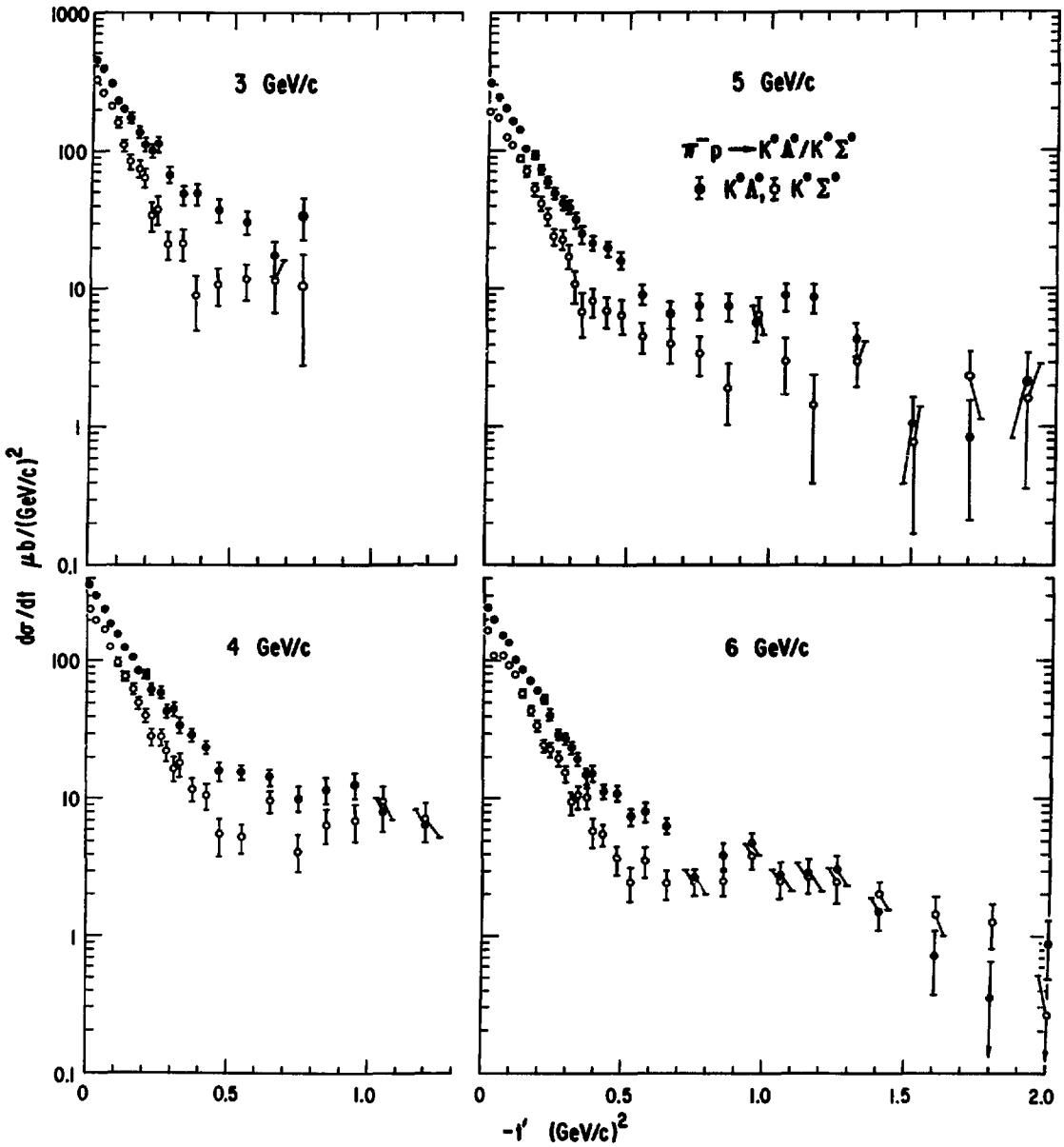
3 GeV/c
5 GeV/c
$\pi^- p \rightarrow K^0\Lambda^0/K^0\Sigma^0$
$K^0\Lambda^0$, $K^0\Sigma^0$
4 GeV/c
6 GeV/c
$d\sigma/dt$ $\mu b/(GeV/c)^2$
$-t'$ $(GeV/c)^2$
1000
100
10
1
0.1
0
0.5
1.0
1.5
2.0

Figure 3

Table 1

Fits of the forward peaks to $d\sigma/dt = Ae^{Bt'}$

$\pi^- p \to K^o \Lambda^o$	-t Interval, $(GeV/c)^2$	Intercept A, $\mu b/(GeV/c)^2$	Slope B, $(GeV/c)^{-2}$
3 GeV/c	0.0 - 0.35	476 ± 14	7.39 ± .28
4 GeV/c	0.0 - 0.35	391 ± 9	7.79 ± .19
5 GeV/c	0.0 - 0.40	333 ± 9	7.95 ± .20
6 GeV/c	0.0 - 0.40	262 ± 6	7.95 ± .17
$\pi^- p \to K^o \Sigma^o$			
3 GeV/c	0.0 - 0.40	371 ± 13	10.07 ± .40
4 GeV/c	0.0 - 0.40	279 ± 8	9.06 ± .25
5 GeV/c	0.0 - 0.40	233 ± 8	9.17 ± .28
6 GeV/c	0.0 - 0.40	176 ± 5	8.56 ± .22

Table 2

Differential Cross Sections in $\mu b/(GeV/c)^2$

3.0 GeV/c		
$-t'$	$d\sigma(\Lambda)/dt$	$d\sigma(\Sigma)/dt$
.0125	438. ±16.	318. ±15.
.0375	380. ±16.	262. ±14.
.0625	301. ±14.	211. ±13.
.0875	225. ±13.	161. ±12.
.1125	202. ±14.	110. ±11.
.1375	171. ±13.	83.7±10.
.1625	137. ±13.	73. 3±10.
.1875	111. ±12.	62. 8±10.
.2125	101. ±12.	34. 4±7. 9
.2375	112. ±14.	37. 5±8. 6
.275	65. 2±8. 1	21. 3±4. 9
.325	47. 9±7. 6	21. 6±5. 3
.375	48. 3±8. 2	8. 8±3. 8
.45	37. 1±5. 6	10. 5±3. 1
.55	30. 4±5. 7	11. 7±3. 6
.65	17. 4±5. 0	11. 4±4. 7
.75	34. 3±11.	10. 7±7. 9

4.0 GeV/c		
.0125	368. ±11.	246. ±9. 7
.0375	302. ±10.	200. ±8. 6
.0625	242. ±8. 8	168. ±7. 9
.0875	186. ±7. 6	127. ±6. 8
.1125	158. ±7. 1	97. 4±6. 1
.1375	125. ±6. 4	75. 6±5. 5
.1625	107. ±6. 1	61. 8±5. 1
.1875	84. 1±5. 6	50. 2±4. 8
.2125	78. 6±5. 7	40. 5±4. 5
.2375	61. 8±5. 3	28. 3±3. 9
.2625	59. 2±5. 5	28. 4±4. 1
.2875	43. 4±4. 8	22. 2±3. 7
.3125	45. 1±5. 1	16. 6±3. 4
.3375	34. 6±4. 6	17. 5±3. 5
.375	29. 1±3. 2	11. 6±2. 2
.425	23. 7±3. 0	10. 4±2. 2
.475	15. 8±2. 6	5. 4±1. 7
.55	15. 5±2. 0	5. 3±1. 2
.65	14. 4±2. 1	9. 6±1. 8
.75	9. 9±1. 9	4. 2±1. 3
.85	11. 3±2. 3	6. 4±1. 8
.95	12. 4±2. 6	6. 9±2. 0
1.05	8. 0±2. 3	9. 6±2. 7
1.20	6. 6±1. 8	7. 1±2. 0

5.0 GeV/c		
$-t'$	$d\sigma(\Lambda)/dt$	$d\sigma(\Sigma)/dt$
.0125	303. ±11.	192. ±10.
.0375	247. ±10.	176. ±9. 7
.0625	204. ±9. 0	129. ±8. 2
.0875	165. ±8. 1	111. ±7. 6
.1125	143. ±7. 5	87. 9±6. 8
.1375	103. ±6. 4	70. 1±6. 1
.1625	94. 3±6. 2	51. 9±5. 3
.1875	71. 5±5. 4	41. 8±4. 8
.2125	58. 8±5. 0	33. 7±4. 4
.2375	48. 9±4. 6	24. 0±3. 9
.2625	41. 8±4. 4	23. 4±3. 9
.2875	39. 4±4. 3	17. 8±3. 5
.3125	31. 5±4. 0	10. 6±2. 9
.3375	24. 8±3. 6	6. 8±2. 4
.375	21. 9±2. 5	8. 1±1. 9
.425	19. 9±2. 6	6. 9±1. 8
.475	16. 1±2. 4	6. 4±1. 8
.55	8. 9±1. 4	4. 5±1. 1
.65	6. 5±1. 3	4. 0±1. 1
.75	7. 4±1. 5	3. 5±1. 1
.85	7. 3±1. 6	1. 95±. 95
.95	5. 7±1. 5	6. 4±1. 7
1.05	8. 7±1. 9	3. 0±1. 3
1.15	8. 5±2. 0	1. 4±1. 0
1.30	4. 4±1. 1	3. 1±1. 1
1.50	1. 01±. 62	. 77±. 61
1.70	. 82±. 71	2. 3±1. 2
1.90	2. 1±1. 3	1. 6±1. 3

6.0 GeV/c		
$-t'$	$d\sigma(\Lambda)/dt$	$d\sigma(\Sigma)/dt$
.0125	245. ±8. 1	161. ±7. 3
.0375	200. ±7. 2	108. ±5. 9
.0625	150. ±6. 1	110. ±5. 8
.0875	133. ±5. 7	91. 2±5. 2
.1125	99. 1±4. 8	77. 9±4. 7
.1375	85. 1±4. 4	58. 4±4. 0
.1625	71. 0±4. 0	43. 8±3. 5
.1875	60. 7±3. 7	34. 3±3. 1
.2125	51. 6±3. 4	24. 2±2. 6
.2375	41. 5±3. 0	23. 0±2. 5
.2625	29. 4±2. 6	19. 9±2. 3
.2875	27. 8±2. 5	15. 3±2. 1
.3125	23. 7±2. 3	9. 4±1. 8
.3375	19. 3±2. 1	10. 3±1. 8
.3625	14. 3±1. 9	10. 2±1. 8
.3875	15. 4±2. 0	5. 8±1. 5
.425	11. 4±1. 2	5. 6±1. 0
.475	11. 0±1. 3	3. 75±. 91
.525	7. 5±1. 1	2. 48±. 77
.575	8. 0±1. 2	3. 56±. 92
.65	6. 41±. 81	2. 44±. 58
.75	2. 67±. 60	2. 55±. 58
.85	3. 90±. 75	2. 51±. 62
.95	4. 81±. 89	3. 95±. 81
1.05	2. 82±. 72	2. 52±. 67
1.15	2. 91±. 77	2. 76±. 73
1.25	3. 10±. 81	2. 47±. 73
1.40	1. 50±. 45	2. 02±. 48
1.60	. 72±. 36	1. 46±. 44
1.80	. 35±. 31	1. 27±. 45
2.00	. 89±. 40	. 26±. 27